Cancer Management and Research

Dovepress

open access to scientific and medical research

Open Access Full Text Article

ORIGINAL RESEARCH

RETRACTED ARTICLE: Inhibition of microRNA-15b-5p Attenuates the Progression of Oral Squamous Cell Carcinoma via Modulating the *PTPN4*/STAT3 Axis

This article was published in the following Dove Press journal:
Cancer Management and Research

Xuerong Liu
Yuanyuan Dong
Dan Song

Department of Oral and Maxillofacial Surgery, Zaozhuang Municipal Hospital, Zaozhuang, Shandong 277100, People's Republic of China

Background: Emerging evidence has demonstrated the important functions of microRNAs (miRNAs) in human malignancies. This study focuses on the function of miR-15b-5p on the oral squamous cell carcinoma (OSCC) progression and the molecules involved.

Methods: Tumor and the paracancerous tissues were obtained from OSCC patients. Differentially expressed miRNAs between tumor and normal tissues were screened out. miR-15b-5p expression in tumors and acquired cells was determined, and its correlation with patient survival was analyzed. Knockdown of miR-15b-5p was introduced in SCC-4 and CAL-27 cells to explore its role in cell growth and metastasis. Binding relationship between miR-15b-5p and *PTPN4* was validated, and altered expression of *PTPN4* was introduced in cells to explore its function in OSCC development. Xenograft tumors were induced in nude mice for in vivo experiments.

Results: miR-15b-5p was abundantly expressed in OSCC tumors and cells and linked to poor survival in patients. Silencing of miR-15b-5p suppressed proliferation, migration, and invasion and triggered apoptosis in SCC-4 and CAL-27 cells. miR-15b-5p targeted *PTPN4*. Further silencing of *PTPN4* blocked the inhibiting functions of miR-15b-5p inhibitor in OSCC cell growth. The in vitro results were reproduced in vivo, where inhibition of miR-15b-5p led to a decline in tumor growth and metastasis in nude mice. *PTPN4* was found as a negative mediator of the STAT3 pathway.

Conclusion: This study evidenced that miR-15b-5p possibly promotes OSCC development through binding to *PTPN4* and the following STAT3 signaling activation. miR-15b-5p may be a potential therapeutic target for OSCC.

Keywords: microRNA-15b-5p, phosphatase non-receptor type 4, signal transducer and activation of transcription 3, oral squamous cell carcinoma

Introduction

Squamous cell carcinoma (SCC) accounts for 90–95% of malignancies in oral mucosa and lip, and oral squamous cell carcinoma (OSCC) remains a life-threatening and distorting disease with a rising incidence of over 300,000 new cases diagnosed annually across the globe, especially in younger generations.[1,2] The incidence of OSCC is particularly high in Asia, which is possibly attributed to the specific lifestyle factors such as chewing of betel quid accompanying with smoking alcohol consumption, human papillomavirus infection and poor oral hygiene.[3] These factors are also closely linked to the dismal survival rate of patients. Thanks to the improvement in diagnosis and therapeutic technologies such as surgical resection, and the adjuvant

Correspondence: Dan Song
Department of Oral and Maxillofacial Surgery, Zaozhuang Municipal Hospital, No. 41 Longtou Road, Shizhong District, Zaozhuang 277100, Shandong, People's Republic of China
Tel/Fax +86-632-3389128
Email Dansong43003@163.com

submit your manuscript | www.dovepress.com
DovePress
http://doi.org/10.2147/CMAR.S272498

radiotherapy and/or chemotherapy, the 5-year survival of patients has seen a notable increase in the past decades, from the 69% in 1990s to 81% in 2000s.[4] Though, the sequela such as local defects, malformations, drug resistance, dysfunction, and the potential recurrence and metastasis risks still burden heavily to the patients.[5] Exploring novel effective and less-invasive treatment strategies is of great importance for OSCC control, which requires more understandings in the mechanical molecules.

MicroRNAs (miRNAs) are the most studied non-coding RNAs in diseases with approximately 22 nucleotides in length, and they exert versatile functions primarily through the post-transcription regulation of the cellular genes that are accountable for multiple essential cellular processes such as cell differentiation and development.[6] They are ideal candidate biomarkers for cancer diagnosis and potential therapeutic targets or tools for many malignancies including OSCC.[7–9] In the present study, a miRNA-based microarray analysis based on the collected tissues from OSCC patients suggested miR-15b-5p as a significantly upregulated one in tumor tissues. miR-15b-5p is a mature miRNA from the 5′-end of pre-miR-15b[10] that has been recognized as an oncogene in several human malignancies such as breast cancer,[11] colon cancer,[12] liver cancer,[13] ovarian cancer[14] and so forth. In SCC, this microRNA was suggested as an indicator of poor tumor differentiation and dismal survival in patients with esophageal SCC.[15] But the exact relevance between miR-15b-5p and OSCC is unknown. Importantly, our integrated bioinformatics analyses suggested phosphatase non-receptor type 4 (*PTPN4*) is a target of miR-15b-5p. *PTPN4* is one of the protein tyrosine phosphatases (PTPs), which are a family of enzymes that remove phosphate groups from proteins hydrolytically with either oncogenic or tumor-suppressing functions demonstrated.[16] Particularly for *PTPN4* itself, its down-regulation by a miRNA was found to lead to metastasis of lung adenocarcinoma-expressing cells.[17] Herein, we speculated that miR-15b-5p possibly triggers OSCC progression through targeting *PTPN4*, with animal and cell experiments performed to validate this hypothesis and explore the potential signaling involved.

Materials and Methods

Ethics Statement

The research was ratified by the Ethics Committee of Zaozhuang Municipal Hospital was performed with the protocols of Declaration of Helsinki. A signed informed consent was received from each participant. The animal experimental protocol was approved by the Committee on the Ethics of Animal Experiments of Zaozhuang Municipal Hospital. All animal procedures were performed in line with the Guide for the Care and Use of Laboratory animals published by the National Institutes of Health, Bethesda, Maryland, USA. Great attempts were made to reduce the usage and suffering in animals.

Sample Collection

Tumor tissues and the paired adjacent normal ones (over 3 cm away from the tumor tissue) were obtained from 37 OSCC patients who were admitted into Zaozhuang Municipal Hospital from January 2014 to April 2016. The pathological stage of patients was confirmed following the Standard issued by the Union for International Cancer Control by two experienced pathologists. The patients were free of a history of preoperative chemotherapy or postoperative adjuvant radiotherapy. The tissues were collected during surgery and instantly preserved at −80°C for further use. The complete clinical information including sex, age, smoking history, alcohol consumption, tumor stage (T1–T4), tumor node metastasis (TNM) stage (I–IV) and lymph node metastasis was collected.

Prognosis Analysis

A three-year follow-up study was performed with a routine examination carried out every three months. The clinical data of patients were collected twice, once in admission and once in discharge. The survival time was defined from the day of recruitment to the day of death or the last-time follow-up. All samples were allocated into two groups according to the median value of miR-15b-5p (2.53). The differences between the two groups were compared by Kaplan-Meier analysis. A Cox proportional hazards model was utilized to analyze the relevance between miR-15b-5p and survival and the 95% confidence interval (CI).

Microarray Analysis

A NanoDrop (ND)-1000 method was used for RNA quantification analysis using tumor and the adjacent tissues from three OSCC patients. The microarray chips and probes were provided by Arraystar Inc (Rockville, MD, USA). RNA was collected using a TRIzol kit (Takara Bio Inc, Japan), amplified and transcribed into cRNA using a Super RNA label kit (Arraystar). The labeled RNA was hybridized onto the Arraystar Human miRNA array V4.0

(8 × 15K, Arraystar). Then, the chips were washed and the array was scanned using a G2505C scanner (Agilent Technologies, CA, USA), and then obtained array images were analyzed using an Agilent Feature Extraction software (version 11.0.1.1). An R Package was used for normalization and subsequent data processing. The RNA with differential expression was screened out with Fold change ≥2.0, $p < 0.05$ and false discovery rate (FDR) <0.05 as the criteria, and the corresponding heatmap was produced.

Reverse Transcription Quantitative Polymerase Chain Reaction (RT-qPCR)

The expression and prognostic value of miR-15b-5p in OSCC were first predicted on The Cancer Genome Atlas (TCGA) database (https://www.cancer.gov/about-nci/organization/ccg/research/structural-genomics/tcga). Again, total RNA was extracted by TRIzol, and the RNA purification was evaluated using a ND-2000 Ultraviolet Spectrophotometer (Thermo Fisher Scientific Inc., Waltham, MA, USA) based on the value of optical density (OD) 260/OD280. Next, the RNA was reversely transcribed to cDNA using a Prime Script RT kit (TaKaRa Bio Inc), and the cDNA quantification was performed on SYBR Premix Ex Taq II. The real-time PCR was conducted using a Light Cycler 480 real-time PCR system. The primers are exhibited in Table 1, with GAPDH and U6 as the internal references. Relative RNA expression was measured by the $2^{-\Delta\Delta Ct}$ method.

RNA in situ Hybridization

The collected tumor tissues were successively fixed, embedded in paraffin, cut into 4-μm sections, dewaxed, and rehydrated. Then, the sections were treated with 15 mg/mL proteinase K (Exiqon, Denmark) at 37°C for 10 min, dehydrated in ethanol, and air-dried. The miR-15b-5p probes were labeled by double-digoxigenin. The U6 snRNA probes were set as positive controls while LNA interfering miRNA probes (Exiqon) as negative controls. The sections were soaked in 50 μL hybridization solution with the addition of 500 ng/mL probes for 18 h of hybridization in a wet box at 37°C. Then, the sections were washed in saline sodium citrate and incubated in 2% goat serum blocking reagent (Roche Ltd, Basel, Switzerland) for 4 h, and then stained with Nuclear Fast Red (Vector Laboratories, USA) for 1 min. The images were scanned using an Aperio Scanscope Virtua (Aperio Scanscope FLGL, Aperio). The staining intensity (SI) and positive proportion (PP) were scored. The scoring for SI was: 0 = blue or light purple (non-staining), and 1 = purple or dark purple. The scoring for PP was: 0 < 35%, 1 ≥ 35%. The tissue staining score = SI score × PP score. A final tissue staining score of 0 was considered as lower expression profile of miR-15b-5p while a score of 1 was regarded as an overexpression profile of miR-15b-5p.

Table 1 Primer Sequences for RT-qPCR

Gene	Primer Sequence (5′-3′)
miR-15b-5p	F: TAGCAGCACATCATGGTTTACA R: TGCGTGTCGTGGAGTC
PTPN4	F: ATCTCCACCGGGAACTCCTA R: CGCTTGGGGAAGTATGAACCA
U6	F: CTCGCTTCGGCAGCACA R: AACGCTTCACGAATTTGCGT
GAPDH	F: CTAAGGCCAACCGTGAAAAG R: ACCAGAGGCATACAGGGACA

Abbreviations: RT-qPCR, reverse transcription quantitative polymerase chain reaction; miR, microRNA; *PTPN4*, phosphatase non-receptor type 4; GAPDH, glyceraldehyde-3-phosphate dehydrogenase; F, forward; R, reverse.

Cell Culture and Transfection

A human immortalized oral epithelial cell line (HIOEC, Bnbio, Beijing, China) and OSCC cell lines (SCC-4, UM-1, CAL-27, OSC-4, ATCC, Manassas, VA, USA) were used. OSCC cells were cultured in DMEM/F-12 (Thermo Fisher) containing 10% fetal bovine serum (FBS) and common antibiotics, while HIOECs were cultured in 10% FBS-supplemented DMEM containing 1% penicillin/streptomycin (Sigma-Aldrich, Chemical Company, St Louis, MO, USA). All cells were cultivated at 37°C in air enriched with 5% CO_2. The specific inhibitor of miR-15b-5p and the inhibitor control, and the small interfering (si) RNA targeting *PTPN4* and the corresponding negative control (NC) were acquired from GenePharma Co., Ltd. (Shanghai, China). The pcDNA 3.1 vectors (Invitrogen, Thermo Fisher) were used as gene carriers. All vectors were transfected into SCC-4 and CAL-27 cells using a Lipofectamine 3000 kit (Thermo Fisher) as per the kit's instructions. A STAT3-specific inhibitor, STAT3-IN-7 (MedChemExpress, Monmouth Junction, NJ, USA), was used for STAT3 inhibition. The transfected cells were further administrated with 5 μm STAT3-IN-7 solution for 48 h of incubation, and then the viability of cells was determined.[18]

Colony Formation Assay

After transfection, cells were sorted in DMEM-contained 60-mm culture dishes at 800 cells/dish for a 10-d incubation with the medium refreshed on the 5th d. After incubation, the cells were fixed by methanol and then stained with 0.5 crystal violet (Sigma-Aldrich) for 10 min, and the number of colonies (over 50 cells) was calculated under a microscope (Olympus Optical Co., Ltd, Tokyo, Japan).

Ki-67 Detection

CAL-27 and SCC-4 cells were sorted in 24-well plates for 48 h or incubation. Next, the cells were fixed in methanol and incubated with anti-Ki-67 (#9449, 1:200, Cell Signaling Technology (CST), USA) at 37°C for 1 h. Next, the cells were incubated with Alexa-488 (Life technologies, USA) at 20°C for 20 min, and then counterstained with 4′, 6-diamidino-2-phenylindole (DAPI, Solarbio Science & Technology Co., Ltd., Beijing, China) for 30 min. The images were obtained using a ProLong Diamond Antifade Mountant (Thermo Fisher), and the Ki-67-positive cells were stained in green.

Transwell Assay

Eight Transwells pre-coated with Matrigel (BD Biosciences, San Jose, CA, USA) were utilized for cell invasion measurement. After 48 h, the transfected cells were resuspended in serum-free DMEM (1×10^5 cells/mL) and loaded into the apical chambers, while the basolateral chambers were loaded with 10% FBS-DMEM. After 24 h, the non-invaded cells were wiped out, while cells invaded to the basolateral chambers were fixed, stained with crystal violet for 15 min, and then observed under the inverted microscope with 5 random fields included. Quantification of cell numbers was conducted using the Image J software (National Institutes of Health, Bethesda, Maryland, USA). The cell migration assay was performed in a similar manner except for pre-coating Matrigel on the apical chambers.

Flow Cytometry

For cell cycle detection, the cells were sorted in 6-well plates (1×10^6 cells per well) and permeated with 75% pre-chilled ethanol at 4°C overnight. After centrifugation at 1000 g for 5 min, the cells were stained with 10 μL propidium iodide (PI, Sigma-Aldrich) solution at 37°C in dark condition for 30 min. The cell cycle was then determined using a flow cytometer (FACScan, BD Biosciences).

Apoptosis of cells was determined using an Annexin V-fluorescein isothiocyanate (FITC) kit (Beyotime Biotechnology Co., Ltd., Shanghai, China). Transfected cells (1×10^6) were resuspended in 195 μL binding buffer containing Annexin V-FITC and PI, and then treated with 5 μL Annexin V-FITC and 10 μL PI for 20 min of incubation in the dark. Then, the percentage of apoptotic cells was measured on the flow cytometer.

Xenograft Tumor in Nude Mice

A total of 24 female specific-pathogen free mice (5 weeks old, 20 ± 2g) were from Vital River Laboratory Animal Technology Co., Ltd. (Beijing, China). SCC-4 and CAL-27 cells with stable transfection (miR-15b-5p inhibitor, miR-15b-5p control, miR-15b-5p inhibitor + si-*PTPN4*, miR-15b-5p inhibitor + si-*PTPN4*-NC) were implanted into the armpit of mice through subcutaneous injection. Then, the tumor size was measured at one-week interval for a total of 4 weeks. The tumor volume (V) was determined as follows: $V = L \times W^2$, where "L" indicates the length while "W" indicates the width. On the 4th week, the mice were euthanized by pentobarbital sodium (150 mg/kg) through intraperitoneal injection. Then, the tumors were taken out and weighed.

Tumor Metastasis in vivo

Another 24 mice were collected for tumor metastasis assay. Cells with stable transfection were implanted into mice through caudal veins (2×10^7 cells per mouse). Eight weeks later, the mice were euthanized in the aforementioned manner, and then the lung tissues of mice were fixed for 2 h and then cut into 5-μm tissue sections for hematoxylin and eosin (HE) staining using a HE staining kit (Solarbio). In brief, the sections were dewaxed, rehydrated, and stained with hematoxylin for 20 min. After differentiation for 30 s, the sections were further stained with eosin solution of 2 min, and the slides were sealed with neutral balsam (Solarbio). The nodules in mouse lung tissues were observed under a microscope (Leica DM500, Germany).

Dual-Luciferase Reporter Gene Assay

The targeting mRNAs of miR-15b-5p were predicted on several bioinformatics systems including TargetScan (http://www.targetscan.org), RNA22 (https://cm.jefferson.edu/rna22), miRanda (https://omictools.com/miranda-tool) and miRDB (http://www.mirdb.org/). The wild-type (WT) sequence of *PTPN4* containing the binding sequence with

miR-15b-5p and the corresponding mutant type (MT) sequence was cloned and inserted into the pMIR-REPORT luciferase vectors (Ambion, Thermo Fisher). HEK293T cells from ATCC were seeded into 6-well plates. Well-constructed luciferase vectors were co-transfected with miR-15b-5p inhibitor or inhibitor control into the HEK293T cells using the Lipofectamine 3000 (Invitrogen). Forty-eight hours later, the luciferase activity was determined using a Dual Luciferase Reporter Gene System 1000 (Promega Corp., Madison, Wisconsin, USA).

Western Blot Analysis

Total protein from cells was extracted using the RIPA cell lysis buffer on ice. The protein concentration was determined by a bicinchoninic acid (BCA) kit (Keygen Biotech Co., Ltd., Jiangsu, China). Thereafter, an equal volume of protein lysates (30 g) was run on 8–12% SDS-PAGE and PVDF membranes (Millipore, Billerica, MA, USA). Then, the membranes were blocked with 5% non-fat milk for 3 h and cultured with anti-STAT3 (ab68153, 1:1000, Abcam Inc., Cambridge, MA, USA), anti-pSTAT3 (ab76315, 1:5000, Abcam) and anti-β-actin (#4970, 1:1000, CST) at 4°C overnight, and further incubated with HRP-labeled goat anti-rabbit secondary antibody at 37°C for 1 h. Then, the protein bands were developed by an enhanced chemiluminescence (ECL) kit (Millipore) and the data were analyzed using an Image Quant LAS-4000 Image Acquisition System (FujiFilm Co., Ltd., Tokyo, China).

Statistical Analysis

SPSS 22.0 (IBM Corp., Armonk, NY, USA) was used for data analysis. Measurement Data were acquired from no less than three independent experiments and exhibited as mean ± standard deviation (SD). The relevance between miR-15b-5p expression and the characteristics of patients was analyzed by the chi-squared test (Sex, smoking and alcohol) and the Kruskal–Wallis test (Metastasis, tumor and TNM stages). A survival curve was produced by Kaplan-Meier analysis, and the survival differences were examined by the Log-rank test. A Cox proportional hazards model was used to analyze the correlation between miR-15b-5p expression and the survival of patients. Differences were analyzed by the *t* test (two groups) and one-way or two-way analysis of variance (ANOVA) followed by Tukey's multiple test (over two groups). The Log-rank test was used for the Post-statistical analyses. *$p < 0.05$ represents statistical significance.

Results

miR-15b-5p is a Potential Prognostic Biomarker for OSCC

The tumor and adjacent normal tissues from three OSCC patients were collected for a miRNA microarray analysis. The results showed that miR-15b-5p was significantly upregulated in tumor tissues compared the paired normal ones (Figure 1A). Then, the expression of miR-15b-5p was first predicted on the TCGA database, which suggested that miR-15b-5p was highly expressed in OSCC tissues (Figure 1B). In addition, the predicted data also suggested patients with high expression of miR-15b-5p showed an unfavorable prognosis (Figure 1C). In consistent with these results, the RT-qPCR also identified an upregulation in miR-15b-5p expression in the collected tumor samples from all patients (Figure 1D). Then, the correlations between the clinical characteristics and miR-15b-5p expression were analyzed. The chi-squared test results showed that the miR-15b-5p expression showed no significant relevance with age ($p = 0.842$), sex ($p = 0.733$), smoking ($p = 0.652$) or alcohol consumption ($p = 0.867$) of patients. But high expression of miR-15b-5p was positively linked to tumor stage, TNM stage, and tumor metastasis (all $p < 0.05$) (Table 2). The miR-15b-5p expression in metastatic and non-metastatic tumor tissues was determined by an RNA in situ hybridization assay, which identified an increase in miR-15b-5p expression in the metastatic tissues (Figure 1E). Further, the association between miR-15b-5p expression and the survival of patients was determined. It was found that higher expression of miR-15b-5p indicated a worse prognosis and shorter survival time in patients (Figure 1F).

Downregulation of miR-15b-5p Suppresses Proliferation of OSCC Cells

Following the findings above, miR-15b-5p expression in HIOEC and the OSCC cell lines (CAL-27, SCC-4, UM-1 and OSC-4) was determined by RT-qPCR. miR-15b-5p was highly expressed in the OSCC cell lines relative to that in HIOECs (Figure 2A). Specifically, the SSC-4 and CAL-27 cell lines with relatively higher miR-15b-5p expression were selected for the subsequent experiments. Thereafter, knockdown of miR-15b-5p was introduced in these two cell lines using the specific miRNA inhibitor and the inhibitor control, and the successful inhibition was confirmed by RT-qPCR (Figure 2B). Next, the colony formation assay

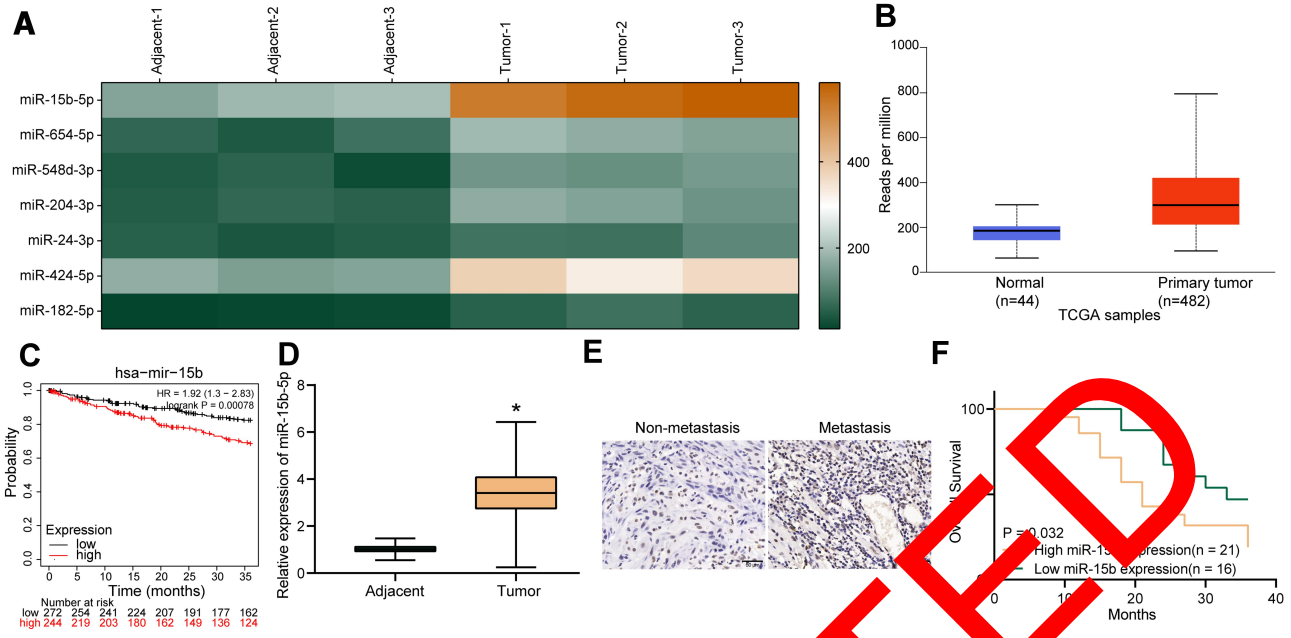

Figure 1 miR-15b-5p is a potential prognostic biomarker indicating OSCC progression. (**A**) differentially expressed miRNAs between tumor tissues and normal tissues from OSCC patients screened out by a microarray analysis (n = 3); (**B**) miR-15b-5p expression in primary OSCC and normal tissues predicted on the TCGA database; (**C**) relevance between miR-15b-5p expression and the survival rate of OSCC patients predicted on the TCGA database; (**D**) miR-15b-5p expression in tumor and normal tissues from all OSCC patients determined by RT-qPCR (n = 37, *$p < 0.05$ according to paired t test); (**E**) miR-15b-5p content in metastatic and non-metastatic tumor tissues was determined by an RNA in situ hybridization assay; (**F**) relevance between miR-15b-5p expression and the survival of patients analyzed by the Kaplan-Meier analysis; high or low miR-15b-5p expression was determined according to the median value (2.53). Repetition = 3.

results showed that the number of formed colonies in an equal given time was notably reduced after miR-15b-5p silencing (Figure 2C). Likewise, miR-15b-5p inhibition led to a decline in Ki-67 expression in cells, indicating a reduction in cell proliferation ability (Figure 2D). Repetition = 3.

Table 2 Correlations Between miR-15b Expression and the Clinicopathologic Characteristics in Patients with OSCC (n = 37)

Characteristics	High miR-15b Expression (n = 21)	Low miR-15b Expression (n = 16)	*p* values
Sex (Male/Female)	12/9	9/7	0.842
Age (Y)	58.63±5.49	59.29±6.13	0.733
Smoking (Yes/No)	8/13	6/10	0.652
Alcohol consumption (Yes/No)	11/10	10/6	0.867
Tumor stage (T1/T2/T3/T4)	3/6/8/4	8/5/3/0	0.046
Clinical TNM stage (I/II/III/IV)	2/4/9/6	9/3/3/1	0.038
Metastasis (Yes/No)	14/7	6/10	0.024

Abbreviations: OSCC, oral squamous cell carcinoma; TNM, tumor node metastasis.

Knockdown of miR-15b-5p Inhibits Migration and Invasion and Blocks Cell Cycle Progression in OSCC Cells

The metastatic potential of cells was further determined. According to the Transwell assays, the numbers of migrated (Figure 3A) and invaded (Figure 3B) cells were notably declined after miR-15b-5p inhibition. Then, the cell cycle progression and apoptosis in SSC-4 and CAL-27 were determined by the flow cytometer. After miR-15b-5p knockdown, the ratio of cells arrested in the G0/G1 phase was increased while that of cells in the S phase was decreased (Figure 3C). As for cell apoptosis, the percentage of apoptotic cells was significantly increased upon miR-15b-5p downregulation (Figure 3D).

Downregulation of miR-15b-5p Suppresses Growth and Metastasis of Xenograft Tumors in Nude Mice

The findings above triggered us to explore whether miR-15b-5p inhibition has a similar effect in vivo. Therefore, SSC-4 or CAL-27 cells with stable transfection of miR-15b-5p inhibitor were implanted into nude mice. It was found that knockdown of miR-15b-5p in cells led to

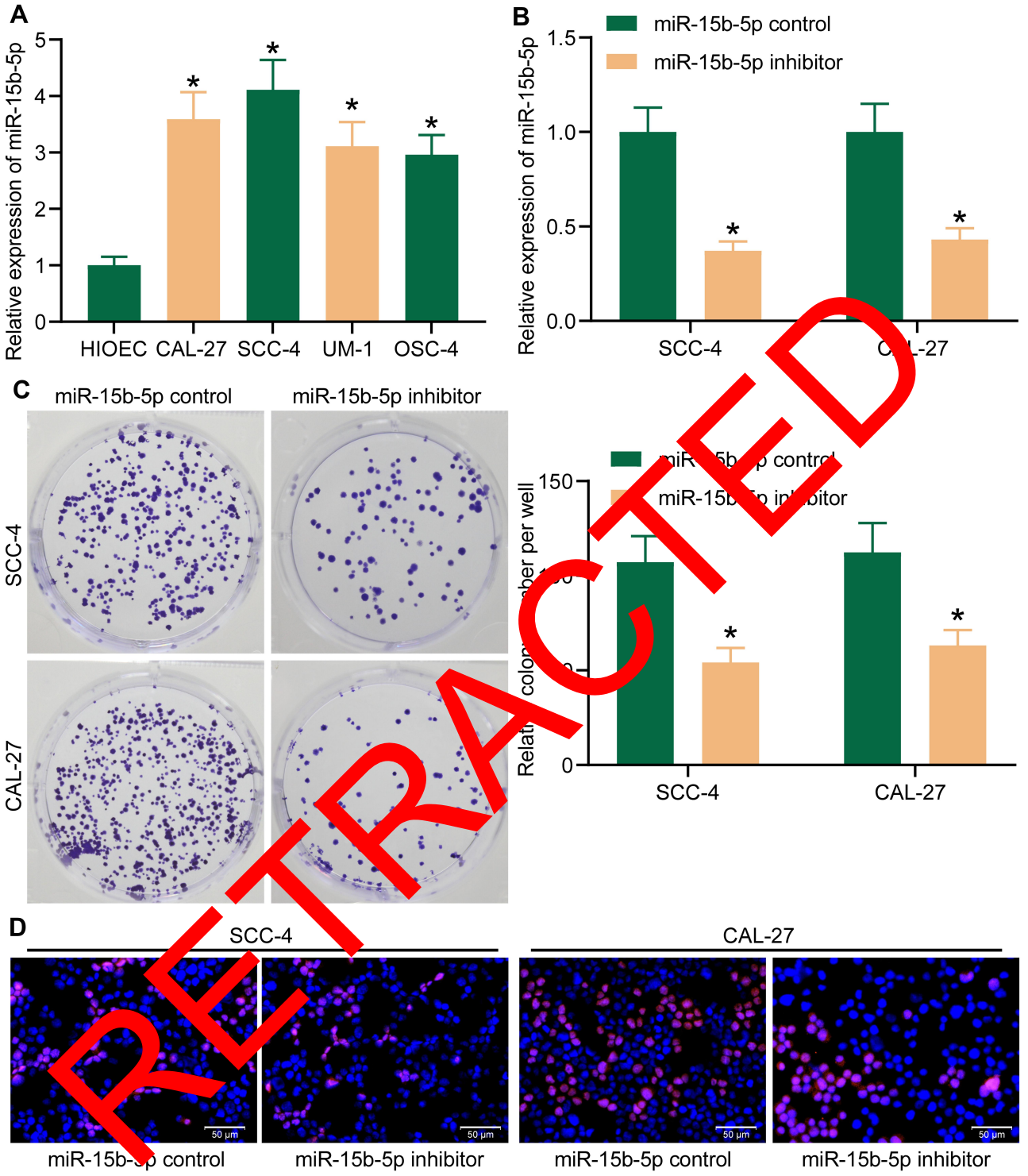

Figure 2 Downregulation of miR-15b-5p suppresses proliferation of OSCC cells. (**A**) miR-15b-5p expression in different cell lines determined by RT-qPCR (*$p < 0.05$ according to one-way ANOVA); (**B**) miR-15b-5p expression in SSC-4 and CAL-27 cells after miR-15b-5p inhibitor transfection determined by RT-qPCR (*$p < 0.05$ according to two-way ANOVA); (**C**) changes in colony formation ability of cells after miR-15b-5p inhibition (*$p < 0.05$ according to two-way ANOVA); (**D**) changes in Ki-67 expression in cells after miR-15b-5p inhibition.

a significant decline in tumor growth rate in mice (Figure 4A). Four weeks later, the tumors were harvested, and miR-15b-5p inhibition in cells was found to result in a decline in tumor weight as well (Figure 4B). In the metastasis assay, mice were implanted with cells through the caudal veins and then euthanized on the 8th week.

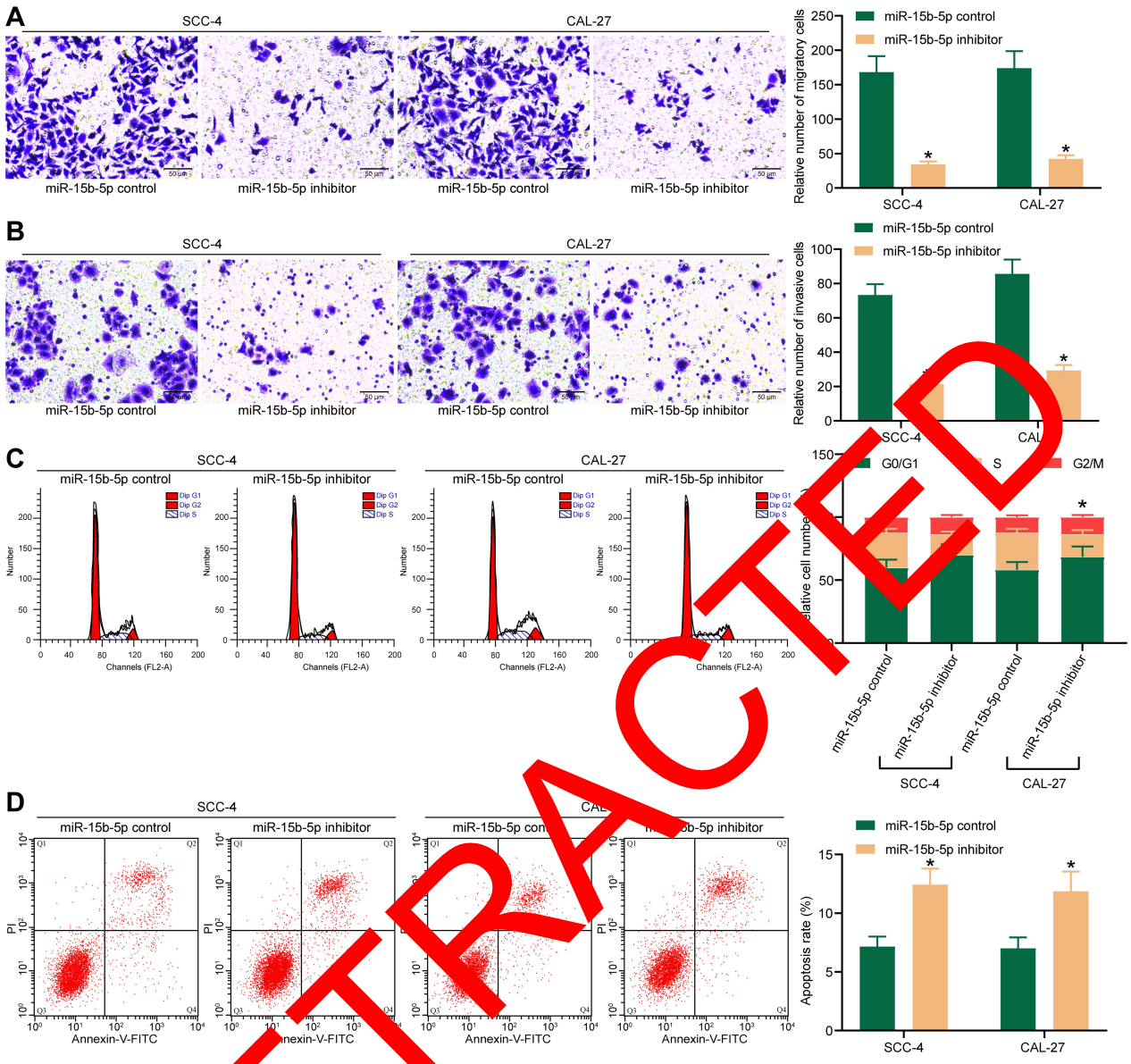

Figure 3 Knockdown of miR-15b-5p inhibits migration and invasion and blocks cell cycle progression in OSCC cells. (**A-B**) migration (**A**) and invasion (**B**) abilities of SSC-4 and CAL-27 cells detected by Transwell assays (*$p < 0.05$ according to two-way ANOVA); (**C-D**) cell cycle progression (**C**) and apoptosis (**D**) in SSC-4 and CAL-27 cells determined by flow cytometry (*p according to two-way ANOVA). Repetition = 3.

Then, the lung tissues were collected for HE staining, which showed that the number of metastatic nodules in lung tissues was notably decreased when miR-15b-5p was suppressed (Figure 4C).

PTPN4 is a Direct Target of miR-15b-5p

An integrated prediction according to data from four bioinformatics systems TargetScan, RNA22, miRanda and miRDB suggested *PTPN4* as a target of miR-15b-5p (Figure 5A). Then, a dual-luciferase reporter gene assay was performed using the putative binding sequences between miR-15b-5p and *PTPN4* predicted on TargetScan, which showed that co-transfection of pMIR-PTN4-WT vector and miR-15b-5p led to an increase in luciferase activity in 293T cells, while cells with MT vector or inhibition control transfection showed no changes in luciferase activity (Figure 5B). Then, the RT-qPCR results identified a decline in *PTPN4* expression in the tumor tissues compared to the adjacent normal ones (Figure 5C), which showed a negative correlation with the miR-15b-5p expression (Figure 5D). Likewise, *PTPN4* was also poorly expressed in the OSCC cell lines and then upregulated in SCC-4 and CAL-27 cells upon miR-15b-5p inhibition (Figure 5E–F). Next, knockdown of *PTPN4* was introduced in SCC-4 and CAL-27 cells (Figure 5G), after

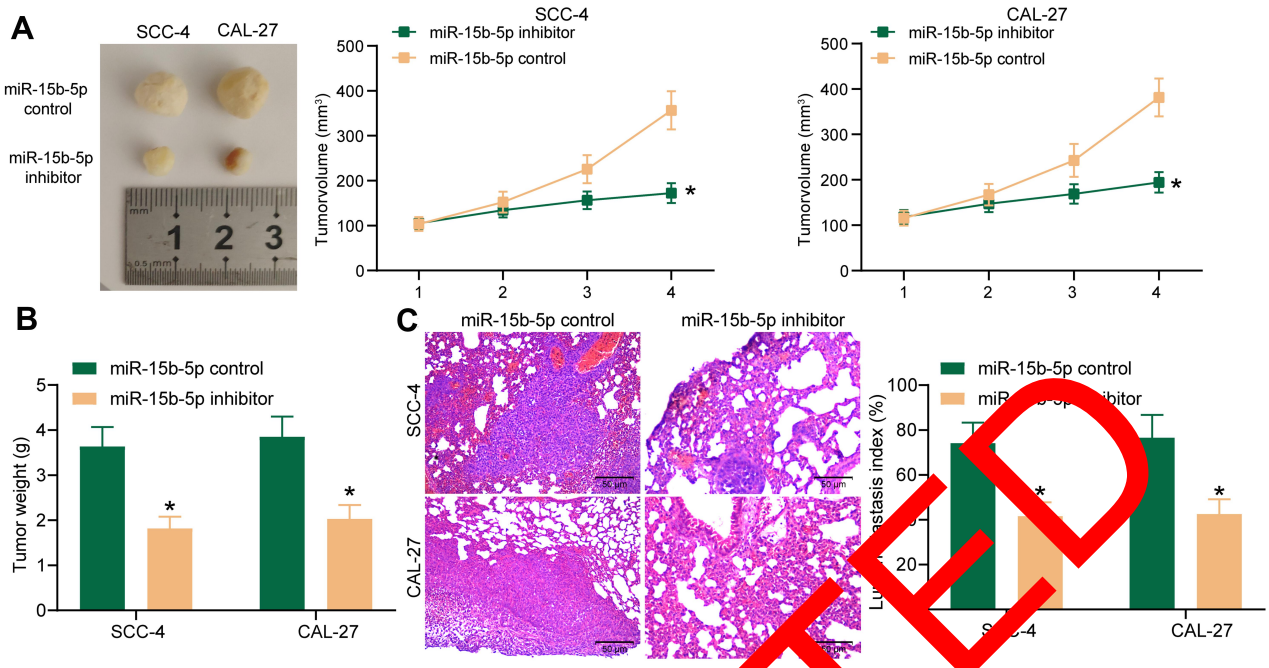

Figure 4 Downregulation of miR-15b-5p suppresses growth and metastasis of xenograft tumors in nude mice. (**A**) weekly changes in tumor volume in mice (*$p < 0.05$ according to two-way ANOVA); (**B**) weight of the xenograft tumors in mice on the 4th week ($p < 0.05$ according to two-way ANOVA); (**C**) number of metastatic nodules in mouse lung tissues observed by HE staining (*$p < 0.05$ according to two-way ANOVA). $N = 3$ in each group. Repetition = 3.

which the apoptosis of cells was notably reduced (Figure 5H). We, therefore, speculated *PTPN4* is a target gene of miR-15b-5p and downregulated during OSCC progression.

Knockdown of *PTPN4* Blocks the Suppressive Roles of miR-15b-5p Inhibitor in OSCC Cells

To further identify the involvement of *PTPN4* in miR-15b-5p-mediated events, knockdown of *PTPN4* was further introduced in SCC-4 and CAL-27 cells in the presence of miR-15b-5p inhibition (Figure 6A). Consequently, it was found that the *PTPN4* expression in cells reduced by miR-15b-5p inhibitor was recovered following *PTPN4* downregulation (Figure 6B). In addition, the increased cell apoptosis was further blocked by si-*PTPN4* as well (Figure 6C). As for the Transwell assays, we noticed that the migration (Figure 6D) and invasion (Figure 6E) rates of SCC-4 and CAL-27 cells suppressed by miR-15b-5p inhibitor were strengthened upon *PTPN4* knockdown.

Co-Transfection of miR-15b-5p Inhibitor and Si-*PTPN4* in OSCC Cells Promotes Tumorigenesis in vivo

The interaction between miR-15b-5p and *PTPN4* was further validated in nude mice. Cells co-transfected with miR-15b-5p inhibitor and si-*PTPN4* were implanted into nude mice, after which we found that the tumor growth rate (Figure 7A) and the tumor weight on the 4th week (Figure 7B) in mice were notably increased compared to those implanted with cells transfected with miR-15b-5p inhibitor and si-NC. As for the in vivo metastasis assay, it was found the number of metastatic nodules in mouse lung tissues was increased when *PTPN4* was further suppressed (Figure 7C). Correlating these results with the findings above, it can be concluded that the suppressive functions of miR-15b-5p inhibitor on tumor growth and metastasis in vivo were diminished by si-*PTPN4*.

PTPN4 is a Negative Regulator of the STAT3 in OSCC Cells

Loss of *PTPN4* has been reported as a contributor to STAT3 activation, which led to further tumor growth of rectal cancer.[19] We therefore speculated if there is a similar regulatory network in OSCC. Then, the STAT3 signaling activity was measured. It was found that the phosphorylation of STAT3 in SCC-4 and CAL-27 was notably increased following *PTPN4* knockdown (Figure 8A). Compared to the that in HIOECs, phosphorylation of STAT3 was increased in the SCC-4 and CAL-27 cells, but the total protein level of STAT3 showed no major

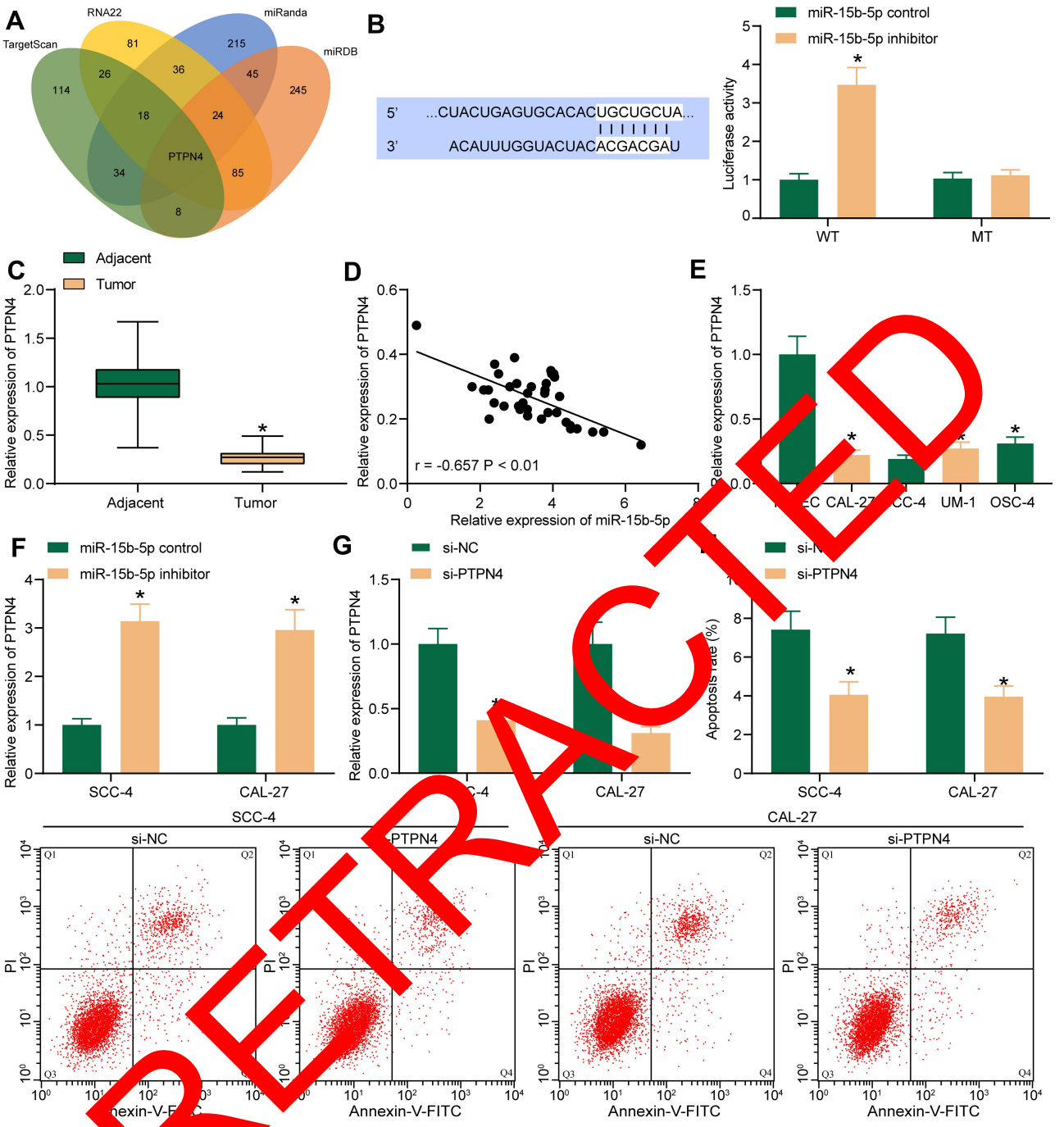

Figure 5 *PTPN4* is a [illegible]t target of miR-15b-5p. (**A**) a Venn diagram for the intersected target gene of miR-15b-5p predicted on four Bioinformatics Systems; (**B**) binding relationship between mi[illegible]5b-5p and *PTPN4* validated by a dual luciferase reporter gene assay (*$p < 0.05$ according to two-way ANOVA); (**C**) mRNA expression of *PTPN4* in tumor and the paired adjace[illegible]issues determined by RT-qPCR (*$p < 0.05$ according to paired *t* test); (**D**) a negative correlation between miR-15b-5p and *PTPN4* expression in OSCCs; (**E**) *PTPN4* expression in HIOECs and OSCC cell lines determined by RT-qPCR (*$p < 0.05$ according to one-way ANOVA); (**F**) *PTPN4* expression in SCC-4 and CAL-27 cells after miR-15b-5p inhibition determined by RT-qPCR (*$p < 0.05$ according to two-way ANOVA); (**G**) mRNA expression of *PTPN4* in cells after si-*PTPN4* administration detected by RT-qPCR (*$p < 0.05$ according to two-way ANOVA); (**H**) apoptosis of cells measured by flow cytometry (*$p < 0.05$ according to two-way ANOVA). Repetition = 3.

differences among the three cell lines (Figure 8B). To further confirm the correlation between STAT3 and *PTPN4*, SCC-4 and CAL-27 cells transfected with si-*PTPN4* were further administrated with the STAT3-specific inhibitor STAT3-IN-7, after which the activity of the STAT3 signaling pathway was decreased (Figure 8C). In this setting, it was found that the apoptosis rate in SCC-4 and CAL-27 cells initially reduced upon *PTPN4* silencing was then increased following STAT3 inhibition (Figure 8D).

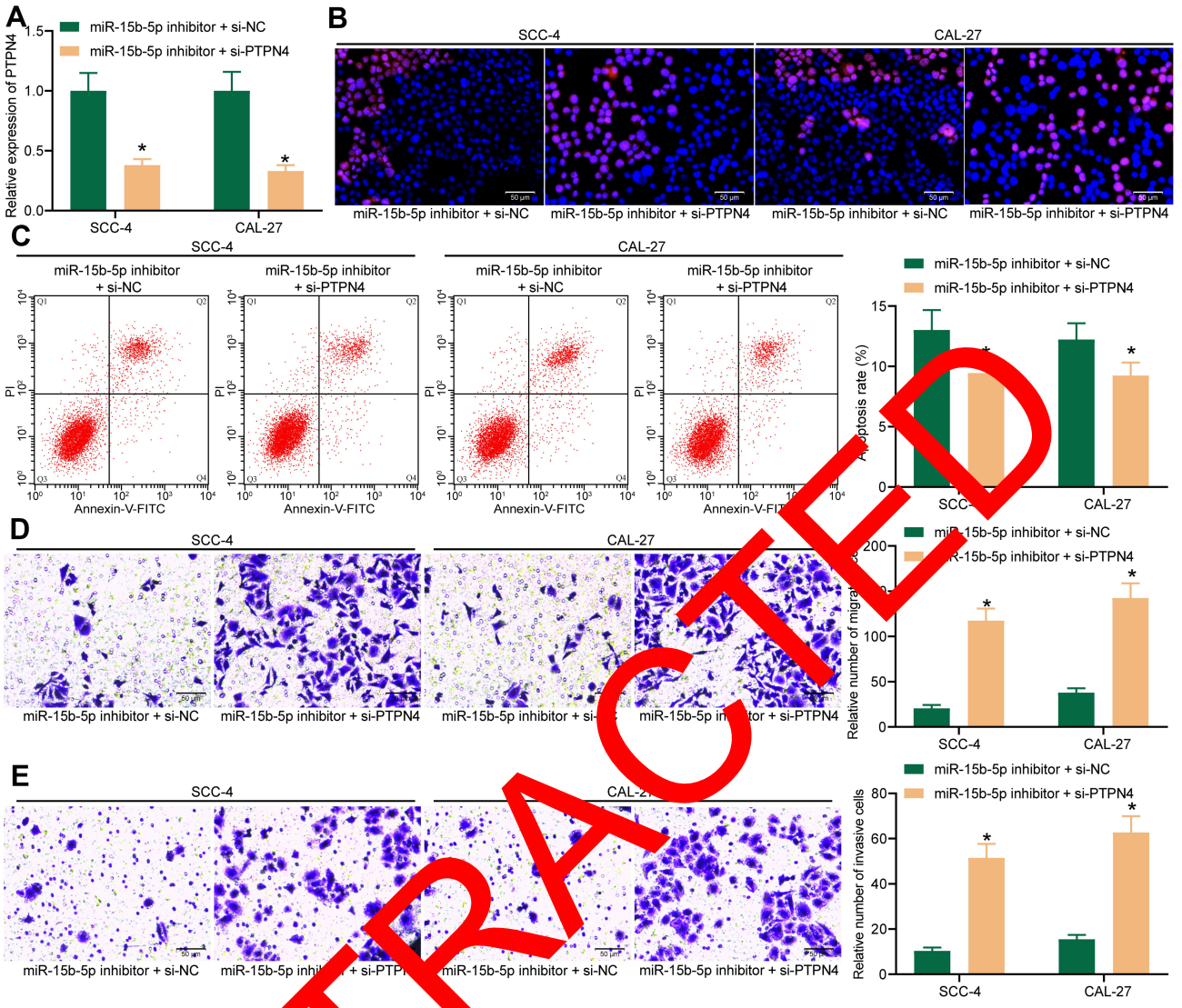

Figure 6 Knockdown of *PTPN4* blocks the suppressive roles of miR-15b-5p inhibitor in OSCC cells. (**A**) mRNA expression of *PTPN4* in SCC-4 and CAL-27 cells after co-transfection of miR-15b-5p inhibitor and si-*PTPN4* determined by RT-qPCR (*p < 0.05 according to two-way ANOVA); (**B**) Ki-67 expression in cells determined by immunofluorescence staining (*p < 0.05 according to two-way ANOVA); (**C**) apoptosis of cells measured by flow cytometry (*p < 0.05 according to two-way ANOVA); (**D-E**) migration (**D**) and invasion (**E**) abilities of cells determined by Transwell assays (*p < 0.05 according to two-way ANOVA). Repetition = 3.

Discussion

Despite the improvements in current therapies, the overall 5-year survival rate of OSCC only improved from 63% to 65% during the last couple of years,[20] which is possibly caused by the frequent recurrence led by local cell metastasis, the failure in early detection, and a lack of drug response to chemotherapies.[21] In the present study, we observed that miR-15b-5p is a potential biomarker for unfavorable prognosis and short survival in patients with OSCC, and inhibition of miR-15b-5p suppressed the malignant behaviors of SCC-4 and CAL-27 cells and inhibited the growth and metastasis of xenograft tumors, during which the *PTPN4* and STAT3 signaling are possibly involved.

Aberrant expression of miRNAs has been well noted to be correlated with the development, metastasis, prognosis and survival of patients with head and neck SCCs (HNSCCs) including OSCC.[22] More specifically, serum miR-625 and miR-5100 are reported as highly accurate prognostic predictors indicating significantly shortened median survival and advanced tumor stages in OSCC patients.[23] In this paper, miR-15b-5p was screened out as a notably increased miRNA in the tumor tissues from patients, and this high-expression profile was validated in all included tissue samples and the acquired cells. Then, miR-15b-5p was found independent of age, sex, smoking, and alcohol consumption in OSCC patients and positively

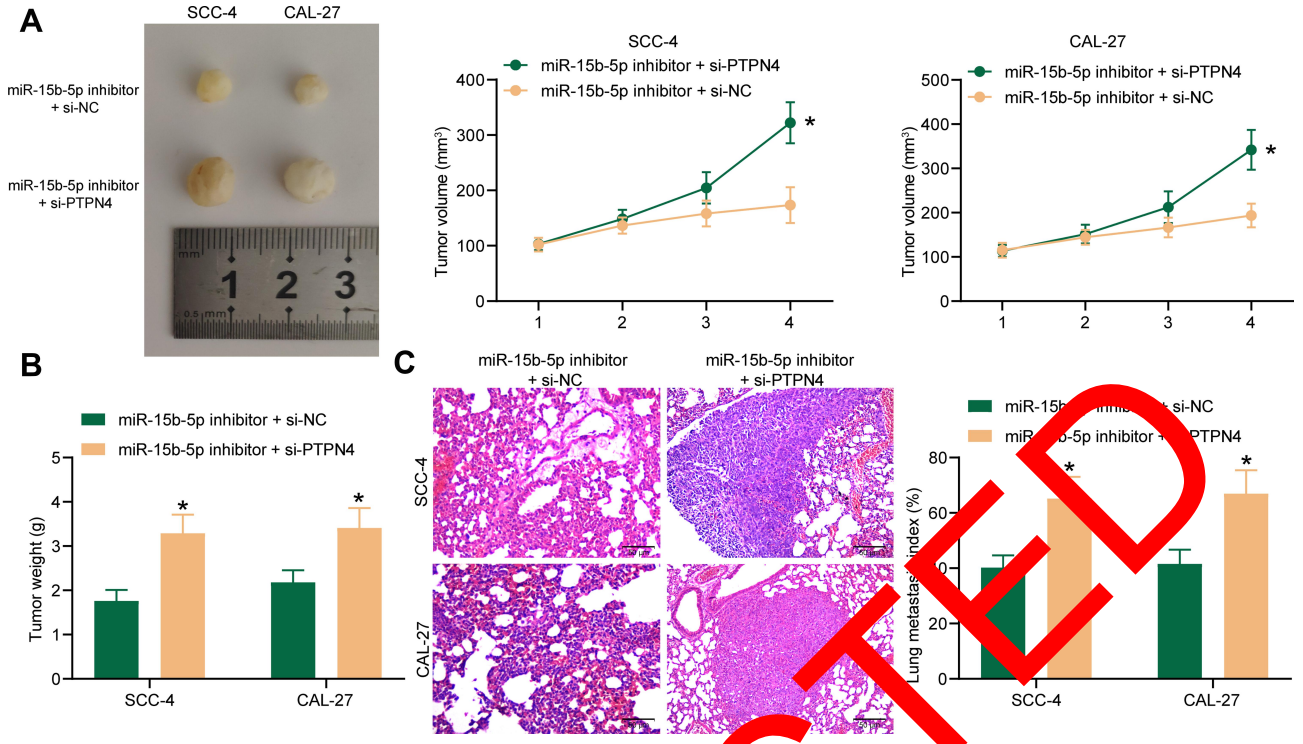

Figure 7 Co-transfection of miR-15b-5p inhibitor and si-*PTPN4* in OSCC cells promote tumorigenesis in vivo. (**A**) weekly tumor size changes in mice after cell implantation; (**B**) tumor weight of each group of mice on the week 4 after mouse euthanasia (*p < 0.05 according to two-way ANOVA); (**C**) metastatic nodules in lung tissues observed by HE staining (*p < 0.05 according to two-way ANOVA). N = 3 in each group. Repetition =

correlated with advanced tumor and clinical TNM stage as well as metastasis. Further, downregulation of miR-15b-5p was introduced in SCC-4 and CAL-27 cells, after which the proliferation, migration, invasion were reduced, while the apoptosis and cell cycle arrest were increased. In a molecular perspective, inhibition of miR-15b-5p was found to suppress expression of Ki67, an important tumor proliferation marker, in these cell lines. Though there has limited evidence concerning the functions of miR-15b-5p in OSCC cells, its downregulation in a colon cancer HT-29 cell line has been reported to be linked to reduced cell growth and increased apoptosis.[12] Likewise, knockdown of miR-15b-5p inhibited growth and invasiveness of two prostate cancer cell lines 22RV1 and PC3.[25] Intriguingly, miR-15b-5p was reported to indicate locoregional relapse in patients with HNSCC underwent intensity-modulated radiotherapy.[26] In addition, the evidence that inhibition of miR-15b-5p suppressed growth and metastasis of xenograft tumors in nude mice further validated the oncogenic role of miR-15b-5p in OSCC.

miRNAs are well known to exert their functions through mediating translation of the diverse downstream mRNAs.[27] In terms of miR-15b-5p, it has been documented as a negative regulator of several transcript targets such as heparanase-2,[11] axis formation inhibitor 2,[13] CDC19,[28] and adipoQ receptor family member3[29] in different cancer types. Here, according to an integrated analysis from the data of four bioinformatics systems, *PTPN4* was suggested as a putative mRNA target of miR-15b-5p. This binding relationship was validated by the subsequent dual-luciferase reporter gene assay. *PTPN4* is a member of the PTPs. PTPs control the phosphotyrosine concentration in signal transduction proteins, which is crucial for normal cell states and is linked to many pathologies once it is lost.[30] Theoretically speaking, PTPs mediate dephosphorylation of proteins, leading to termination of signaling pathways and the subsequent inhibition of cell proliferation, growth and differentiation, and either anti-oncogenic or oncogenic phosphatases have been found.[16] Two PTP members PTP receptor R (PTPRR) and PTP receptor-type, Z polypeptide 1 (PTPRZ1) were found as indicators for increased tumor differentiation and favorable survival rate in patients with OSCC.[31] Here, silencing of *PTPN4* was introduced in cells with stable transfection of miR-15b-5p inhibitor, after which the malignant behaviors suppressed by miR-15b-5p inhibition were recovered. The similar anti-oncogenic role of *PTPN4* has been reported in rectal cancer, where low expression of *PTPN4*

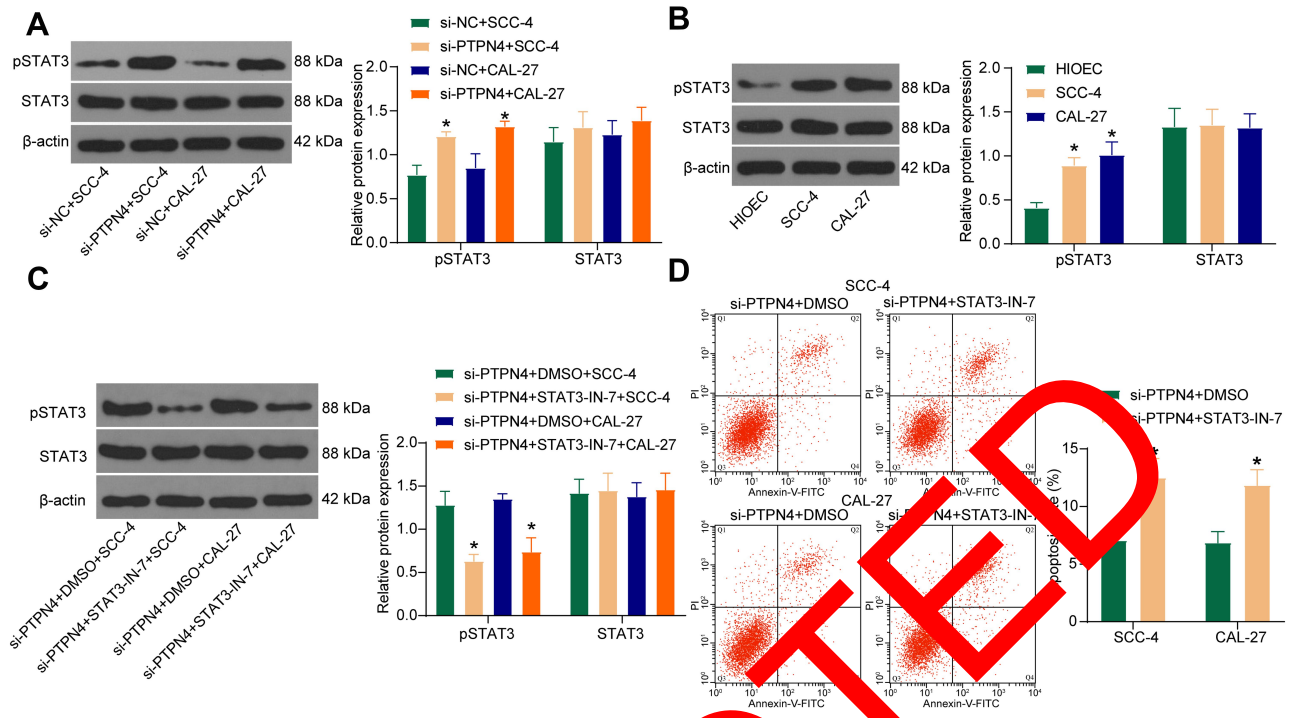

Figure 8 *PTPN4* is a negative regulator of the STAT3 in OSCC cells. (**A**) protein expression and phosphorylation of STAT3 in cells transfected with si-*PTPN4* determined by Western blot analysis (*$p < 0.05$ according to two-way ANOVA); (**B**) protein expression and phosphorylation of STAT3 in HIOEC, SCC-4 and CAL-27 cells determined by Western blot analysis; (**C**) protein expression and phosphorylation of STAT3 in SCC-4 and CAL-27 cells after further STAT3-IN-7 treatment determined by Western blot analysis (*$p < 0.05$ according to two-way ANOVA); (**D**) apoptosis rate in SCC-4 and CAL-27 cells determined by flow cytometry (*$p < 0.05$ according to two-way ANOVA). Repetition = 3.

was correlated with dismal prognosis in patients, while upregulation of *PTPN4* suppressed renal cancer growth and promoted cell cycle arrest through targeting the STAT3 signaling pathway.[19] STAT3 is a frequently over-expressed transcription factor of the STAT members and regulates a large number of oncogenic genes governing the growth and metastasis of tumor cells, thus may serve as a target for cancer prevention and treatment.[32] Here, we noticed that the phosphorylation of STAT3 was high in the SCC-4 and CAL-27 cells and further increased following knockdown of *PTPN4* as well. Likewise, aberrant expression of STAT3 has also been noted to be involved in the progression of HNSCCs including OSCC.[33,34] Hence, activation of this signaling pathway is possibly responsible for miR-15b-5p- and si-*PTPN4*-mediated events.

To conclude, this study evidenced that miR-15b-5p exerts an oncogenic role in OSCC in both cells and animals through directly binding to *PTPN4* and the following STAT3 phosphorylation. This study may offer novel insights into OSCC control. However, the exact involvement of STAT3 in this network requires more convincing evidence. We would like to perform further rescue experiments to validate its implication. Also, we hope more studies will be carried out in this field to reduce the burden of OSCC and other malignancies.

Funding

There is no funding to report.

Disclosure

The authors declare no conflict of interest.

References

1. Panarese I, Aquino G, Ronchi A, et al. Oral and Oropharyngeal squamous cell carcinoma: prognostic and predictive parameters in the etiopathogenetic route. *Expert Rev Anticancer Ther*. 2019;19(2):105–119.
2. Thomson PJ. Perspectives on oral squamous cell carcinoma prevention-proliferation, position, progression and prediction. *J Oral Pathol Med*. 2018;47(9):803–807. doi:10.1111/jop.12733
3. Yu-Duan T, Chao-Ping W, Chih-Yu C, et al. Elevated plasma level of visfatin/pre-b cell colony-enhancing factor in male oral squamous cell carcinoma patients. *Med Oral Patol Oral Cir Bucal*. 2013;18(2):e180–186. doi:10.4317/medoral.18574
4. Amit M, Yen TC, Liao CT, et al. Improvement in survival of patients with oral cavity squamous cell carcinoma: an international collaborative study. *Cancer*. 2013;119(24):4242–4248. doi:10.1002/cncr.28357

5. Liu L, Chen J, Cai X, Yao Z, Huang J. Progress in targeted therapeutic drugs for oral squamous cell carcinoma. *Surg Oncol*. 2019;31:90–97. doi:10.1016/j.suronc.2019.09.001
6. Fahey C, Angelini C, Flory SL. Grass invasion and drought interact to alter the diversity and structure of native plant communities. *Ecology*. 2018;99(12):2692–2702. doi:10.1002/ecy.2536
7. Dumache R. Early diagnosis of oral squamous cell carcinoma by salivary microRNAs. *Clin Lab*. 2017;63(11):1771–1776. doi:10.7754/Clin.Lab.2017.170607
8. Gomes CC, de Sousa SF, Gomez RS. MicroRNAs: small molecules with a potentially role in oral squamous cell carcinoma. *Curr Pharm Des*. 2013;19(7):1285–1291.
9. Zhang H, Li T, Zheng L, Huang X. Biomarker MicroRNAs for diagnosis of oral squamous cell carcinoma identified based on gene expression data and MicroRNA-mRNA network analysis. *Comput Math Methods Med*. 2017;2017:9803018.
10. Sun W, Lan J, Chen L, et al. A mutation in porcine pre-miR-15b alters the biogenesis of MiR-15b\16-1 cluster and strand selection of MiR-15b. *PLoS One*. 2017;12(5):e0178045.
11. Wu B, Liu G, Jin Y, et al. miR-15b-5p promotes growth and metastasis in breast cancer by targeting HPSE2. *Front Oncol*. 2020;10:108.
12. Gasparello J, Gambari L, Papi C, et al. High levels of apoptosis are induced in the human colon cancer HT-29 cell line by co-administration of sulforaphane and a peptide nucleic acid targeting miR-15b-5p. *Nucleic Acid Ther*. 2020;30(3):164–174. doi:10.1089/nat.2019.0825
13. Dong Y, Zhang N, Zhao S, Chen X, Li F, Tao X. miR-221-3p and miR-15b-5p promote cell proliferation and invasion by targeting Axin2 in liver cancer. *Oncol Lett*. 2019;18(6):6491–6500.
14. Miao S, Wang J, Xuan L, Liu X. LncRNA TTN-AS1 acts as sponge for miR-15b-5p to regulate FBXW7 expression in ovarian cancer. *Biofactors*. 2020;46(4):600–607. doi:10.1002/biof.1622
15. Li CY, Zhang WW, Xiang JL, Wang XH, Li J, Wang [illegible]. Identification of microRNAs as novel biomarkers for esophageal squamous cell carcinoma: a study based on The Cancer Genome Atlas (TCGA) and bioinformatics. *Chin Med J (Engl)*. 2019;132(18):2213–2222. doi:10.1097/CM9.0000000000000[illegible]
16. Bollu LR, Mazumdar A, Savage MI, Brown PH. Molecular pathways: targeting protein tyrosine phosphatases in cancer. *Clin Cancer Res*. 2017;23(9):2136–2142. doi:10.1158/10[illegible]-0432.CCR-16-0934
17. Zhu C, Deng X, Wu J, et al. MicroRNA-[illegible] promotes migration and invasion of CD133(+)/CD326(+) lung adenocarcinoma initiating cells via *PTPN4* inhibition. *Tumour Biol*. 2016;37(8):11289–11297. doi:10.1007/s13277-016-4955-8
18. Liu CY, Tseng LM, Su JC, et al. Novel sorafenib analogues induce apoptosis through SHP-1-dependent STAT3 inactivation in human breast cancer cells. *Breast Cancer Res*. 2013;15(4):R63. doi:10.1186/bcr3457
19. Zhang BD, Li Y, Zhang LD, Wang YY, Liu HY, Jia BQ. Loss of *PTPN4* activates STAT3 to promote the tumor growth in rectal cancer. *Cancer Sci*. 2019;110(7):2263–2272.
20. Zou B, Li [illegible], Xu K, et al. Identification of key candidate genes and pathways in tongue squamous cell carcinoma by integrated Bioinformatics analysis. *Exp Ther Med*. 2019;17(5):4089–4099.
21. Ishida K, Tomita H, Nakashima T, et al. Current mouse models of oral squamous cell carcinoma: genetic and chemically induced models. *Oral Oncol*. 2017;73:16–20. doi:10.1016/j.oraloncology.2017.07.028
22. Masood Y, Kqueen CY, Rajadurai P. Role of miRNA in head and neck squamous cell carcinoma. *Expert Rev Anticancer Ther*. 2015;15(2):183–197. doi:10.1586/14737140.2015.978294
23. Shi J, Bao X, Liu Z, Zhang Z, Chen W, Xu Q. Serum miR-626 and miR-5100 are promising prognosis predictors for oral squamous cell carcinoma. *Theranostics*. 2019;9(4):920–931. doi:10.7150/thno.30339
24. Menon SS, Guruvayoorappan C, Sakthivel KM, Rasmi RR. Ki-67 protein as a tumour proliferation marker. *Clin Chim Acta*. 2019;491:39–45. doi:10.1016/j.cca.2019.01.011
25. Chen R, Sheng L, Zhang HJ, Ji M, Qian W[illegible]. miR-15b-5p facilitates the tumorigenicity by targeting RECK and predicts tumour recurrence in prostate cancer. *J Cell Mol Med*. 2018;22([illegible]):1855–1863. doi:10.1111/jcmm.13469
26. Ahmad P, Sana J, Slavik M, et al. MicroRNA-15b-5p predicts locoregional relapse in head and neck carcinoma patients treated with intensity-modulated radiotherapy. *Cancer Genomics Proteomics*. 2019;16(2):139–146. doi:10.21873/cgp.20119
27. Iwakawa HO, Tomida Y. The functions of MicroRNAs: mRNA decay and translational repression. *Trends Cell Biol*. 2015;25(11):651–665. doi:10.1016/j.tcb.2015.07.011
28. Wang F, Zu Y, Zhu [illegible], et al. Long noncoding RNA MAGI2-AS3 regulates CDC19 expression by sponging miR-15b-5p and suppresses bladder cancer progression. *Biochem Biophys Res Commun*. 2018;507(1–4):231–235. doi:10.1016/j.bbrc.2018.11.013
29. Zhao C, Li Y, Chen G, Wang F, Shen Z, Zhou R. Overexpression of miR-15b-5p promotes gastric cancer metastasis by regulating PAQR4. *Oncol Rep*. 2017;38(1):352–358. doi:10.3892/or.2017.5673
30. Hendriks W, Bourgonje A, Leenders W, Pulido R. Proteinaceous inhibitors and inhibitors of protein tyrosine phosphatases. *Molecules*. 2018;23:2. doi:10.3390/molecules23020395
31. Dus-Szachniewicz K, Wozniak M, Nelke K, Gamian E, Gerber H, Ziolkowski P. Protein tyrosine phosphatase receptor R and Z1 expression as independent prognostic indicators in oral squamous cell carcinoma. *Head Neck*. 2015;37(12):1816–1822. doi:10.1002/hed.23835
32. Chai EZ, Shanmugam MK, Arfuso F, et al. Targeting transcription factor STAT3 for cancer prevention and therapy. *Pharmacol Ther*. 2016;162:86–97. doi:10.1016/j.pharmthera.2015.10.004
33. Geiger JL, Grandis JR, Bauman JE. The STAT3 pathway as a therapeutic target in head and neck cancer: barriers and innovations. *Oral Oncol*. 2016;56:84–92. doi:10.1016/j.oraloncology.2015.11.022
34. Mali SB. Review of STAT3 (Signal Transducers and Activators of Transcription) in head and neck cancer. *Oral Oncol*. 2015;51(6):565–569. doi:10.1016/j.oraloncology.2015.03.004